Utilization of remote sensing and GIS for land use and land cover mapping in Wasit province, Iraq

Meena K. Abdulkareem*, and *Hussein* Sabah Jaber

University of Baghdad, College of Engineering, Department of Surveying, Baghdad, Iraq

Abstract. All physical components on the Earth's surface are collectively termed land cover, such as water, vegetation, bare soil, and artificial structures made by humans. In contrast, land use refers to how humans use the land for urban growth, agricultural practices, and commerce activities. The increase in population density has resulted in changes in land use/land cover (LULC) because of urban expansion and other human activities. This study investigates the effectiveness of a supervised MLC classification algorithm to produce LULC maps of Wasit Governorate from multiple satellite images using remote sensing and GIS techniques, which is of great importance for earth observation applications, such as environmental monitoring and disaster prediction. Three Landsat 8-9/OLI satellite images were used to cover the entire study area for the year 2024. Preprocessing including radiometric and atmospheric corrections was performed using ENVI 5.3V software, and mosaicking, layer stacking, and image subsetting were performed using Arc GIS 10.8 to improve image quality. Image processing was performed using ENVI 5.3V to find LULC classes using the Maximum Likelihood (MLC) algorithm. The results indicated five LULC classifications in the study area: vegetation, water bodies, built-up areas, arid areas and saline areas. Furthermore, post-processing of the images, including accuracy assessment, was performed to assess the accuracy of the LULC mapping, yielding an overall agreement of 90.58% and a Kappa index of 88%, which measures the extent of agreement or accuracy. These results are convincing with a kappa index of more than 0.8. This study demonstrates the potential of Landsat 8-9/OLI images integrated with machine learning methods for efficient land use classification, analysis and monitoring. This study also provides broad horizons of knowledge for planners and regional authorities.

1 Introduction

LULC play an important role in many aspects, such as environmental monitoring, agricultural production, disaster prediction and urban development. Remote sensing techniques through satellite imaging have become one of the most important technologies used all over the world, and they are essential for producing LULC maps with accurate

* Corresponding author: mina.abd2412m@coeng.uobaghdad.edu.iq

classifications. Classification of LULC is critical to environmental, cultural and political research, as it is the basis for government oversight that contributes to achieving sustainable livelihoods in line with modern ecosystems. Remote sensing, in combination with GIS, provides advanced tools for managing and monitoring modern ecosystems [1]. Landsat 8 was launched in February 2013 through a collaboration between NASA and the U.S. Geological Survey (USGS), providing high-spectral coverage and spatial resolution data [2].in September 2021, Landsat 9 was launched to improve the quality of Landsat 8 data [3] .Several studies have highlighted the high capabilities of Landsat 8,9 data in LULC maps classification. A study conducted by [4] showed the effectiveness of Landsat 8,9 satellites in mapping LULC. The study's findings by demonstrated that LULC mapping is used to identify urban growth and changes in arid regions, agricultural areas, and waterways. Additionally, the Landsat imagery utilized aids in creating GIS maps that precisely depict the distributions of evaporation, precipitation, river levels, discharge, temperature, and dust storms[5]. Researchers' studies [6], [7] have highlighted the benefits of using Landsat 8 to monitor LULC, especially when related to managing archaeological and heritage sites. This study discussed the importance of using modern technologies represented by remote sensing and GIS to find maps of LULC and its changes and monitor them instead of using traditional surveying methods because they are expensive and complicated and require more effort, especially if the study area has a large area, as remote sensing technologies and GIS are considered the most efficient in terms of shortening time, effort and cost and providing more excellent coverage through satellite images and can find classifications of LULC maps for a large area such as the study area represented by Wasit Governorate, which lacks previous studies in this regard. This study aims to demonstrate the use of remote sensing and GIS in producing and analyzing LULC maps for Wasit province and assess the accuracy of classification of these maps using the Kappa coefficient.

2 Methods

2.1 Study area

The province of Wasit is situated in the eastern portion of the central area of Iraq, between latitudes 31° 52′ and 33° 36′ and longitudes 44° 30′ and 46° 40′ (Figure 1). Numerous provinces, including Baghdad, Diyala, Babil, Al-Qadisiyah, DhiQar, and Maysan, are its neighbours. It shares an eastern border with Iran State. The province of Wasit possesses abundant natural resources, including oil and water. Other significant sectors of the economy include trade and farming. The capital of the Wasit governorate, situated on the Tigris River, is Al-Kut City. With a total area of 17889.09 km2, the Wasit Governorate makes up 4% of Iraq's total land area. With limited rainfall and high temperatures, it is categorized as a coastal region with a climate between the Mediterranean and hot, arid deserts [8]

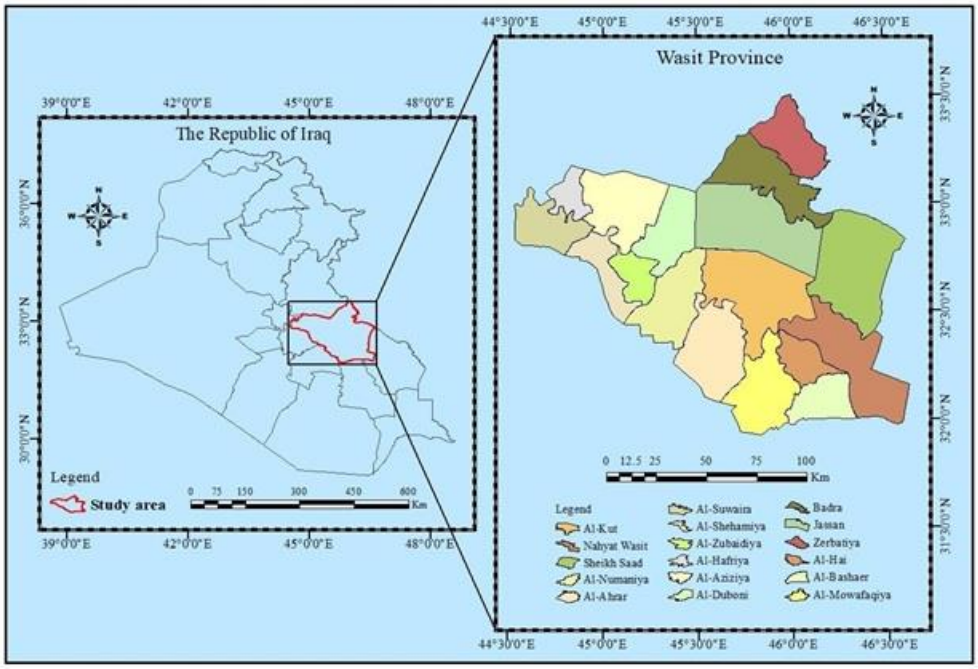

Fig. 1. Study area map.

2.2 Materials

Landsat 8-9/OLI images were used in this study since they were accessible and had a spatial resolution of 30 meters. Three images of the study area were gathered and pre-processed to correct atmospheric and radiometric errors. Figures (2,3,4, and 5) show images collected by the USGS in September 2024, which are cloud-free.

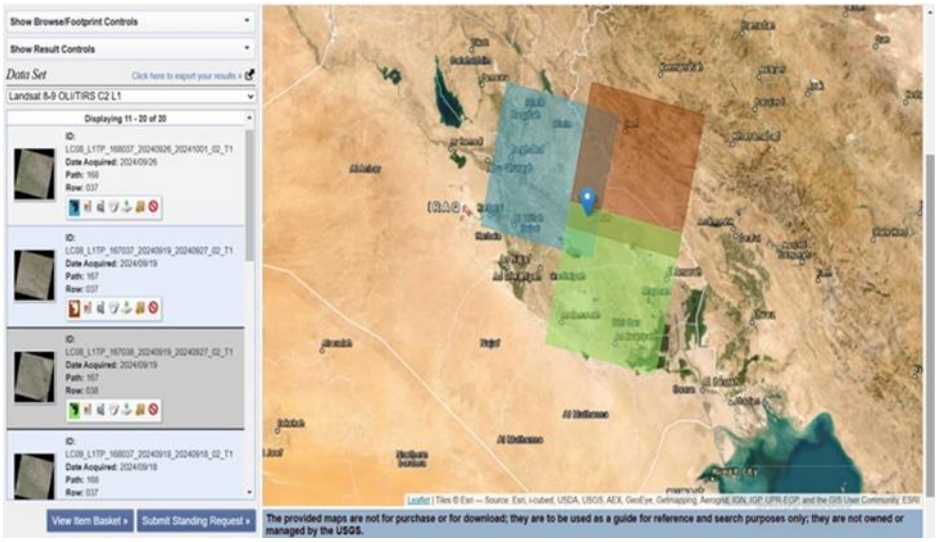

Fig. 2. USGS website.

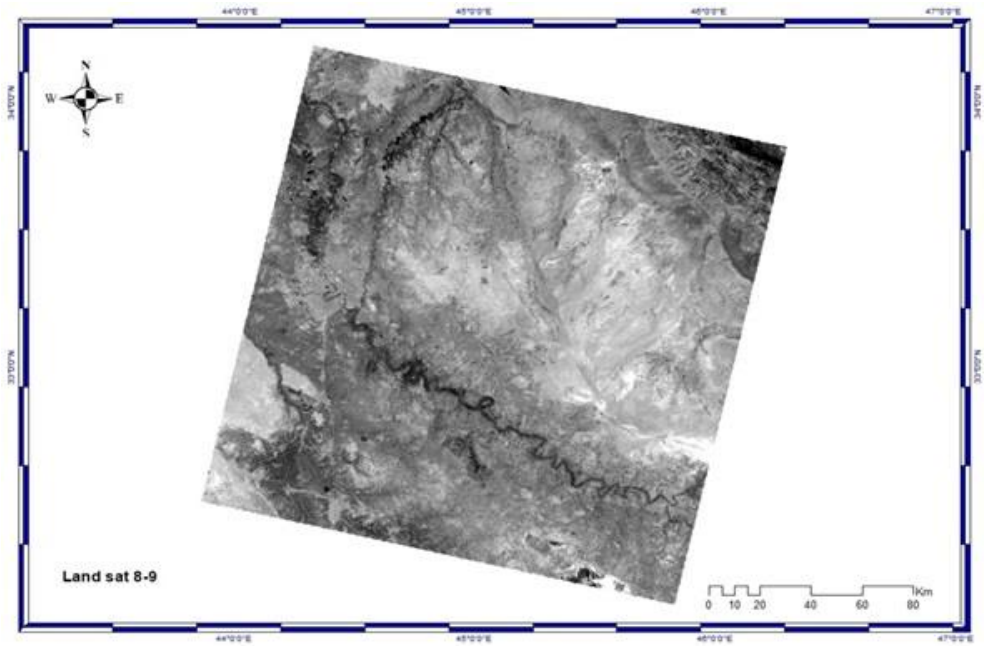

Fig. 3. Landsat 8-9 OLI image (1) (USG).

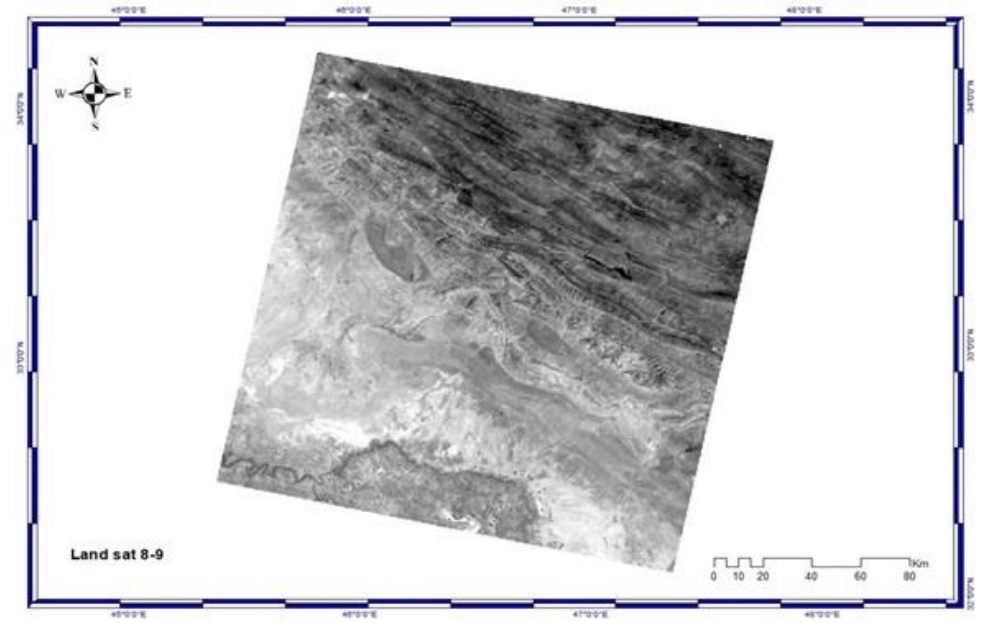

Fig. 4. Landsat 8-9 OLI images (2)(USGS).

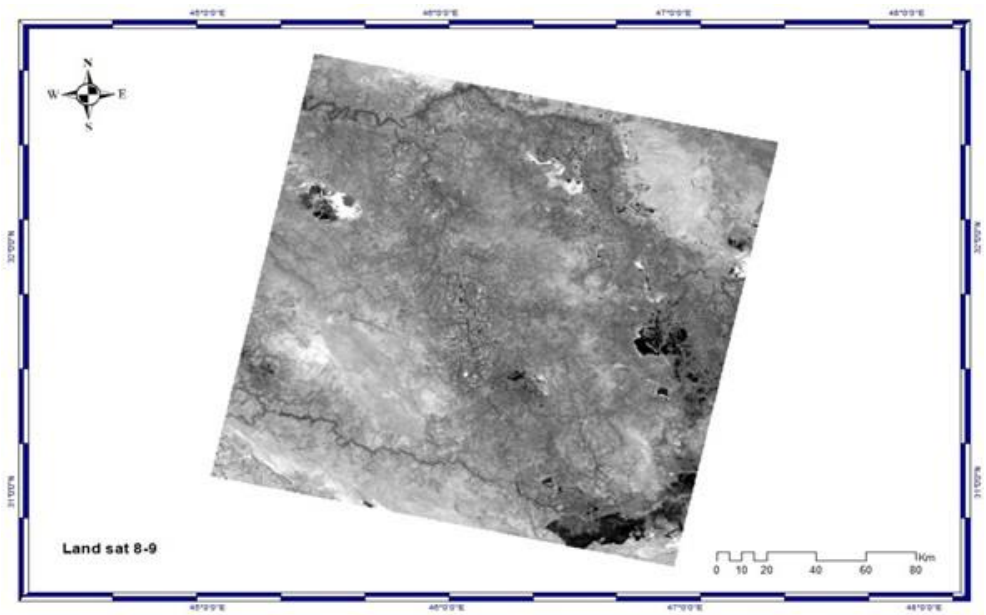

Fig. 5. Landsat 8-9 OLI images (3)(USGS).

2.3 Methodology of Research

This study employs a series of processing stages using remote sensing and GIS, as illustrated in Figure (6).

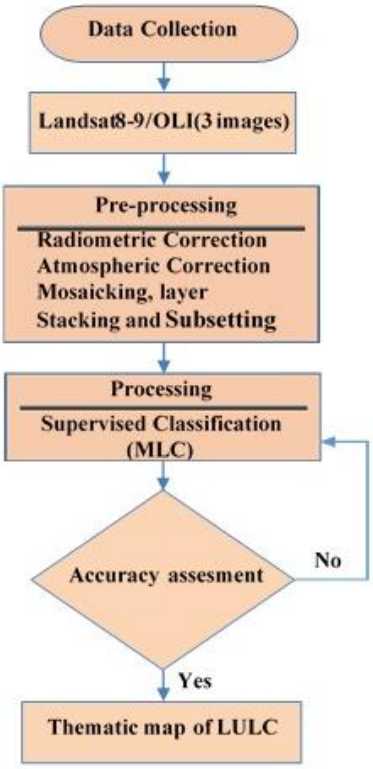

Fig. 6. The diagram of the research methodology.

2.3.1 The procedure of mosaicking satellite imagery

Upon completing the layer stacking procedure, which consolidates all bands into a singular file for enhanced accessibility inside the application, the processing is further refined using the composite band tool in ArcGIS 10.8 software [9], [10]. The metadata specifies a standard coordinate system, which is then used for image mosaicking, as illustrated in Figure (7).

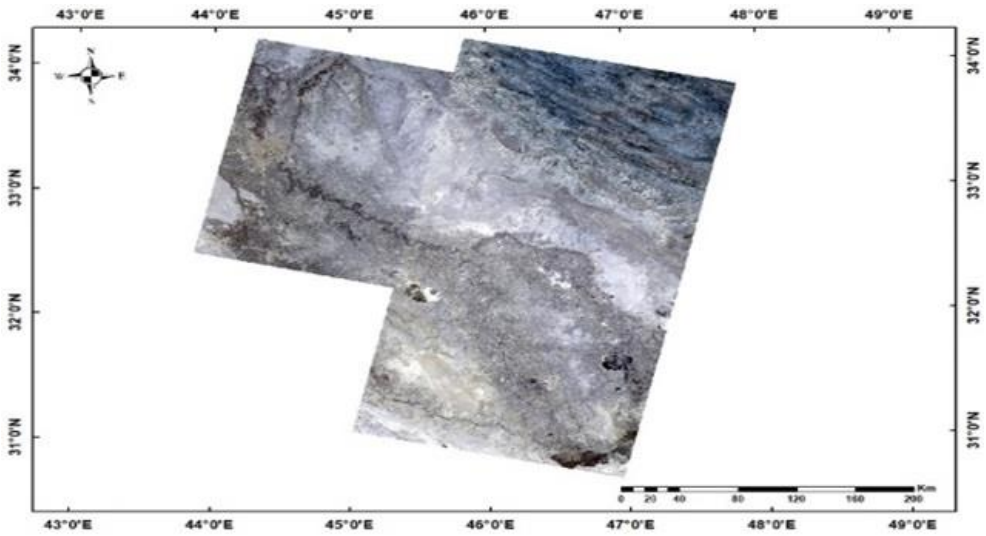

Fig. 7. Mosaiking Landsat 1-2-3 images for the study area.

2.3.2 The procedure of sub-setting satellite imagery

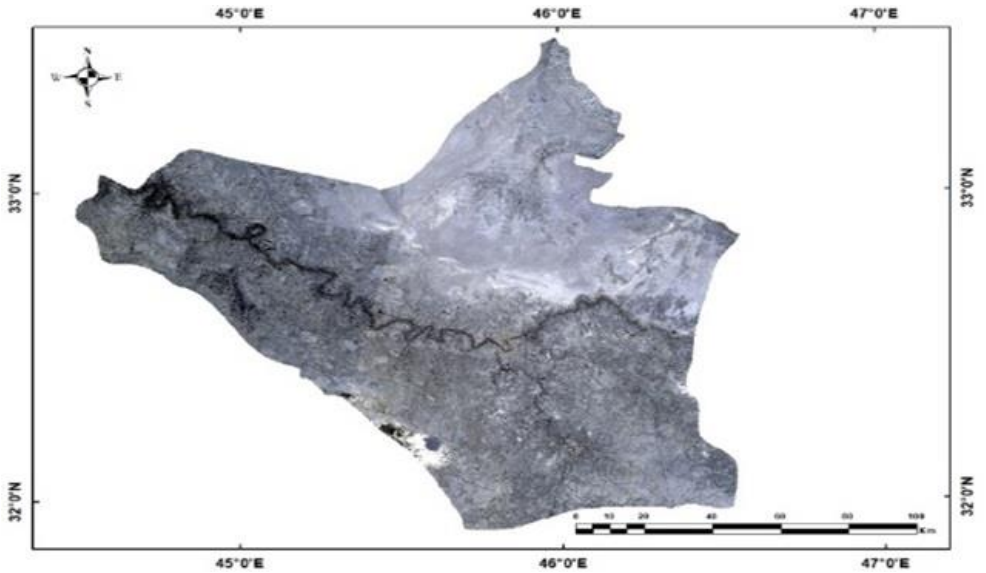

Fig. 8. Image after subsetting.

2.3.3 The Maximum Likelihood Classifier (MLC)

The MLC assumes that the data to be categorized follows a Gaussian or normal distribution. It uses training data to determine the categories' means, variances, and covariances, which are then used to evaluate probabilities. This method considers the mean values and the variation in brightness values within each category when assigning

classifications[11]. The MLC algorithm is an effective classification method as it has the ability for a quantitative consideration of several classes and spectral bands simultaneously[12], [13]. as seen in the equation below [14] :

$$g_i(x) = ln\ \rho(\omega i) - ½\ ln|\sum i| - ½\ (x - m_i)^T \sum^{-1}(x - m_i) \quad (1)$$

Where

i: Category.

x: Data of n-dimensional (n*:* the number of bands).

p(ωi): The probability that category ωi happens in the image.

$|\Sigma_i|$: The determinant of the covariance matrix of category ωi data.

Σ_i^{-1}: The matrix inverse.

m_i: Mean vector.

Envi 5.3's Region of Interest (ROI) tool was used to gather the training data. Additionally, ROIs were randomly constructed as pixel-based validation data to assess accuracy.

2.3.4 Performance evaluation strategies

To ensure the reliability of the classification results, the last step in processing satellite images is to evaluate the accuracy of the classification. This is done by comparing the results of the classification model with reference data that accurately illustrate the groups of LULC classifications. The first stage of accuracy assessment is to collect original accurate data in specific areas which show the groups of LULC classifications. This information can be provided either through factual information obtained from field surveys or from other reliable methods, such as high-quality images and maps. A confusion matrix is then created. This tabular representation compares the classification results to the source data, and multiple accuracy measurements can then be made from the data in the confusion matrix.[15]. Producer's accuracy is calculated by dividing the total number of pixels identified in a category by the total number of pixels in that category identified by ground reference data (i.e., the column total) [14]:

$$\text{Producer's accuracy for class j} = \frac{x_{jj}}{x_{+j}} \quad (2)$$

The user's accuracy is the ratio of the accurate pixel count in a category to the overall pixel count categorized within that class[14]:

$$\text{User's accuracy for class i} = \frac{x_{ii}}{x_{i+}} \quad (3)$$

Overall accuracy (OA) is defined as the proportion of accurately categorized pixels to the total pixel count in the image. To calculate this, divide the total number of accurately categorized pixels (i.e., the diagonal sum of the error matrix) by the total number of pixels within the image(N) [14]:

$$OA = \frac{\sum_{i=1}^{k} x_{ii}}{N} \quad (4)$$

The Kappa index is an important indicator that evaluates the degree of concordance between observed and anticipated classifications while considering the likelihood of agreement occurring by chance [14]:

$$K = \frac{N\sum_{i=1}^{k} x_{ii} - \sum_{i=1}^{k}(x_{i+} \times x_{+j})}{N^2 - \sum_{i=1}^{k}(x_{i+} \times x_{+j})} \quad (5)$$

Where:

N= Total number of observations

k = The number of rows in the error matrix

$x$ii=The number of observations in row i and column i

xi+= The marginal totals for row i

x+j = The marginal totals for column j

The Kappa index value ranges from (zero to one). Zero indicates a significant disparity between the categorization outputs and the reference findings. There is strong agreement that the precision is moderate if the value is equal to 1 and ranges from 0.4 to 0.8. The lower value correlates with a stochastic categorization.

3 Results and discussion

3.1 Findings from thematic map classifications

Supervised classifications of images were conducted using the MLC algorithm in ENVI 5.3v. The classification results have been transformed into shapefiles for use in ArcGIS 10.8v, enabling the development of the LULC thematic maps, which are categorized under five principal categories depending on visual analysis and field observations of the studied area: Built-up, vegetation, saline, barren, and water bodies, as illustrated in Figure (9).

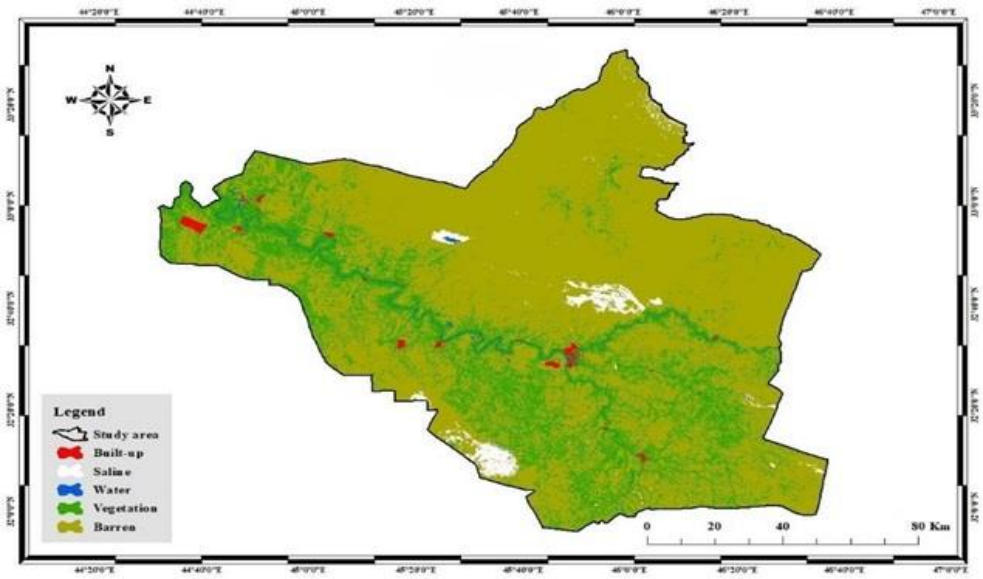

Fig. 9. LULC Thematic map utilizing MLC.

3.2 The results of area computations with percentage allocations for classes

Table (1) displays the area computation and each class's percentages. At more than 69.86%, most of the class reported a barren area. Only 1.63% of the total area came from water sources, primarily rivers and branches; another 0.82% came from built-up areas. The

vegetation class had the second-highest percentage at 27.24 %. Soil area accounted for almost 0.45% of the total but covered more than 80.16 km^2 in the actual Area.

Table 1. Computation of area and percentage of classes.

Class	Area(km^2)	Percent %
Barren	12496.71	69.86%
Vegetation	4874.13	27.24%
Water	290.79	1.63%
Built-up	147.30	0.82%
Saline	80.16	0.45%
Total	17889.09	100%

3.3 Evaluation of Classification Accuracy and Verification Results

Upon concluding the classification process using ENVI 5.3v software, the accuracy of the algorithm-generated images was assessed and validated. The results showed approval, as the Kappa index was more than 0.8. Table (2) below displays the confusion matrix of five classes in the studied area. MLC classification produced an overall accuracy of 90.85% and a kappa index of 0.88 (Table 2). Table 2 indicates that around 12,000 samples were selected for each of the five classes in the research area, with a distribution of 2,400 samples per class, to methodically and thoroughly represent the region. Three classes had the highest degree of misclassification utilizing the MLC. The barren area has a deficient user accuracy of 75.04%, and approximately 25% of pixels identified as barren areas were misclassified, specifically vegetation, water bodies, built-up areas, and saline areas. The vegetation had a user accuracy of 88.09%, which is considered low. The pixels identified as vegetation were, in fact, urban areas, water bodies, saline regions, and, to a lesser extent, barren areas. The built-up class has a high misclassification rate, with a producer accuracy of only 70.39 %. This means that approximately 30% of the examined pixels selected as built-up were mistakenly classified as other categories, such as vegetation, barren areas, saline areas, and particularly water bodies. Saline regions exhibit the highest producer's accuracy among all categories. 99.38%. Conversely, water bodies exhibit superior user accuracy compared to other categories (100%).

Table 2. Confusion matrix of the MLC approach.

Actual Data (in pixels)							
Class	**Built-up**	**Saline**	**Water**	**Vegetation**	**Barren**	**Total**	**User's accuracy**
Built-up	7438	0	0	7	229	7674	96.92%
Saline	4	10538	85	0	116	10743	98.09%
Water	0	0	10021	0	0	10021	100%
Vegetation	133	20	397	10427	859	11836	88.09%
Barren	2991	45	6	76	9375	12493	75.04%
Total	10566	10603	10509	10510	10579	52767	
Producer's accuracy	70.39%	99.38%	95.35%	99.21%	88.6%		
Overall accuracy = (5311/5863) =90.58%							
Kappa Index for Agreement = 0.88							

The evaluation of land use map classification accuracy using the MLC algorithm is deemed satisfactory since the Kappa index exceeds 0.8.

4 Conclusions

This study adds to the existing body of knowledge by examining the efficacy of a supervised MLC classification algorithm to extract LULC maps from Wasit City satellite images by applying GIS and remote sensing. With a kappa score of 0.88 and an overall accuracy of 90.85%, the results demonstrate the efficacy of extracting LULC from satellite images using the MLC method and calculating its class areas. The study outcomes ensure the examined region's sustainability and can be utilized for environmental monitoring, water resource management, and urban planning. To determine the best, it is necessary to continue testing these methods using many categories of LULC and satellite images. It is recommended that the MLC algorithm be used to detect LULC and create a geodatabase by integrating remote sensing and GIS for all areas of Iraq. The results can be compared with different classification techniques.

References

1. M. M. Kadhim, “Monitoring land cover change using remote sensing and GIS techniques: a case study of Al-Dalmaj marsh, Iraq,” Journal of Engineering **24(9)**, 96–108 (2018), DOI: 10.31026/j.eng.2018.09.07
2. E. Chuvieco, *Fundamentals of Satellite Remote Sensing: An Environmental Approach* (CRC Press, 2020), DOI: 10.1201/9780429506482
3. J. G. Masek, J. R. Irons, A. L. M. MacDonald, C. E. Justice, S. J. Hook, "Landsat 9: Empowering open science and applications through continuity," Remote Sens. Environ. **248**, 111968 (2020), DOI: 10.1016/j.rse.2020.111968
4. Shahfahad, S. S. Ghosh, A. Ahmad, A. Rahman, "Comparative evaluation of operational land imager sensor on board Landsat 8 and Landsat 9 for land use land cover mapping over a heterogeneous landscape," Geocarto Int. **38(1)**, 2152496 (2023), DOI: 10.1080/10106049.2022.2152496
5. L. K. Abbas, "Mapping land cover/land use for change derivation using remote sensing and GIS technique," Iraqi J. Sci. **62(10)**, 3772–3778 (2021), DOI: 10.24996/ijs.2021.62.10.35
6. F. A. Zwain, T. T. Al-Samarrai, Y. I. Al-Saady, "A study of desertification using remote sensing techniques in Basra Governorate, south Iraq," Iraqi J. Sci. **62(3)**, 912–926 (2021), DOI: 10.24996/ijs.2021.62.3.22
7. H. S. Abbas, A. S. Mahdi, "Study of desertification using remote sensing imagery in south Iraq," Iraqi J. Sci. **60(4)**, 904–913 (2019), DOI: 10.24996/ijs.2019.60.4.24
8. A. Sahar, *Change detection for some land cover types of Wasit Province (Eastern Iraq) using remote sensing and GIS techniques for years 1989–2017* (2018)
9. M. H. Al-Helaly, I. A. Alwan, A. N. AL-Hameedawi, "Environmental investigation of Bahar Al-Najaf region using Sentinel-2 images," Engineering and Technology Journal **40(4)**, 732–742 (2022), DOI: 10.30684/etj.v40i5.2245
10. H. B. Ghalib, A. B. Al-Hawash, W. S. Al-Qurnaw, B. H. Sultan, A. W. Al-enzy, "Marshes waters sources hydrochemistry of the Bahr Al-Najaf at Najaf Province, Iraq," J. Phys.: Conf. Ser. **1279**, 012059 (2019), DOI: 10.1088/1742-6596/1279/1/012059
11. R. S. Dwivedi, *Remote Sensing of Soils* (Springer, 2017), DOI: 10.1007/978-3-662-53740-4
12. J. S. Alawamy, S. K. Balasundram, A. H. Mohd. Hanif, C. T. Boon Sung, "Detecting and analyzing land use and land cover changes in the region of Al-Jabal Al-Akhdar,

Libya using time-series Landsat data from 1985 to 2017," Sustainability **12(11)**, 4490 (2020), DOI: 10.3390/su12114490

13. S. Mushtaq, S. Saleem, R. Ahmed, M. S. Tass, J. A. Rather, G. M. Rather, "Spatio-temporal analysis land use land cover changes in South Kashmir region of North-western Himalayas using Landsat data," Discover Geoscience **2(1)**, 37 (2024), DOI: 10.21203/rs.3.rs-3830014/v1
14. E. Miranda, A. B. Mutiara, W. C. Wibowo, "Classification of land cover from Sentinel-2 imagery using supervised classification technique (preliminary study)," in *2018 International Conference on Information Management and Technology (ICIMTech),* IEEE, 69–74 (2018), DOI: 10.1109/ICIMTech.2018.8528122
15. H. A. Abbas, H. S. Jaber, A. D. Salman, "Land use mapping from Sentinel satellite imagery using remote sensing and GIS techniques," in IOP Conf. Ser.: Earth Environ. Sci. **1374**, 012042 (2024), DOI: 10.1088/1755-1315/1374/1/012042